ACS APPLIED MATERIALS & INTERFACES

Research Article

www.acsami.org

Time-Resolved Study on Xanthene Dye-Sensitized Carbon Nitride Photocatalytic Systems

Huiyu Zhang, Shuang Li, Rong Lu, and Anchi Yu*

Department of Chemistry, Renmin University of China, Beijing 100872, People's Republic of China

Supporting Information

ABSTRACT: Dye sensitization is a promising strategy to extend the visible light absorption of carbon nitride (C_3N_4) and increase the photocatalytic hydrogen evolution efficiency of C_3N_4 under visible light irradiation. However, the interaction dynamics between C_3N_4 and a sensitized dye has not been reported in the literature. Herein, we selected four commonly used xanthene dyes such as fluorescein, dibromofluorescein, eosin Y, and erythrosine B and prepared their corresponding dye-sensitized-C_3N_4 composites. For the first time, we derived the electron transfer rate from the LUMO of each photoexcited xanthene dye to the conduction band of C_3N_4 using picoesecond time-resolved fluorescence measurements. We also obtained the reduction potentials of all selected xanthene dyes and C_3N_4 with cyclic voltammetry measurements. The cyclic voltammetry measurements gave a consistent result with the picosecond time-resolved fluorescence measurements. Besides, the possibility of the selected xanthene dye as an acceptor for the hole of the photoexcited C_3N_4 was also discussed. We believe this study is significant for the researcher to understanding the fundamental aspects in the xanthene dye-sensitized-C_3N_4 photocatalytic systems.

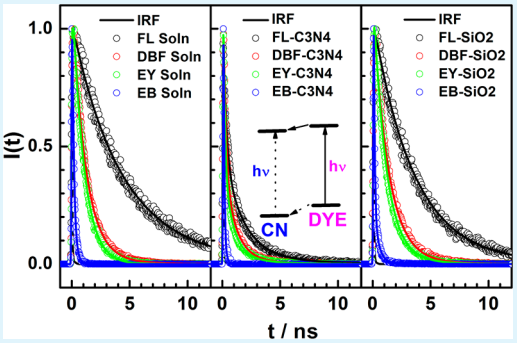

KEYWORDS: *xanthene dye, carbon nitride, electron transfer, hole transfer, dye-sensitized photocatalytic system*

INTRODUCTION

To efficiently convert the solar energy into hydrogen energy, a semiconductor photocatalyst needs to have the capability of absorbing longer wavelength light while still having a suitable band edge to cover the water redox potential.[1−4] Carbon nitride (C_3N_4), a metal-free photocatalyst, has attracted great attention due to its successful applications in water splitting under visible light irradiation.[5−11] However, it still exhibits relatively low photocatalytic hydrogen evolution activity under visible light irradiation because of its relatively large band gap (~2.7 eV).[12−15] Recent studies showed that the dye sensitization is a promising strategy to extend the visible light absorption of C_3N_4 and increase the photocatalytic hydrogen evolution efficiency of C_3N_4 under visible light irradiation.[16−24]

In 2010, Takanabe et al. reported that the C_3N_4 sensitized with magnesium phthalocyanine can display a stable photocatalytic hydrogen evolution activity and it has an apparent quantum efficiency of 0.07% at 660 nm.[16] More recently, Peng and co-workers found that the zinc phthalocyanine derivatives can also be used as sensitizers for graphitic C_3N_4 and the apparent quantum efficiency of the C_3N_4 sensitized with zinc phthalocyanine derivatives is larger than that with magnesium phthalocyanine.[17−20] Besides, Min and Lu reported that the C_3N_4 sensitized with eosin Y has an apparent quantum efficiency of 19.4% at 550 nm.[21] Meanwhile, Wang et al. reported that the thin layer C_3N_4 sensitized with erythrosine B has an apparent quantum efficiency of 33.4% at 460 nm.[22] Most of these studies are focused on how to improve the photocatalytic hydrogen evolution activity of C_3N_4 sensitized with dyes under visible light irradiation; however, the dynamics of the interaction between a dye and C_3N_4 in the dye-sensitized-C_3N_4 systems has not been studied.

In this contribution, we sensitized C_3N_4 with four commonly used xanthene dyes such as fluorescein, dibromofluorescein, eosin Y, and erythrosine (Scheme 1) and determined the electron transfer rate from the LUMO of each selected

Scheme 1. Molecular Structures of Fluorescein, Dibromofluorescein, Eosin Y, Erythrosine B, and Carbon Nitride

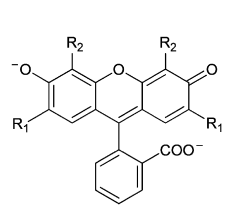

Fluorescein	$R_1 = R_2 = H$
Dibromofluorescein	$R_1 = H$, $R_2 = Br$
Eosin Y	$R_1 = R_2 = Br$
Erythrosine B	$R_1 = R_2 = I$

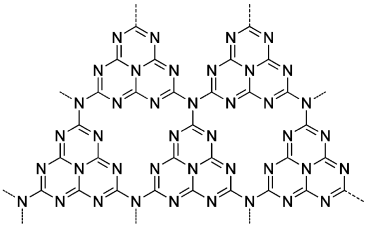

Carbon Nitride

Received: July 13, 2015
Accepted: September 21, 2015
Published: September 21, 2015

DOI: 10.1021/acsami.5b06309
ACS Appl. Mater. Interfaces 2015, 7, 21868−21874

photoexcited xanthene dye to the conduction band of C_3N_4 with picosecond time-resolved fluorescence measurements. We also measured the reduction potential of each selected xanthene dye and C_3N_4 with cyclic voltammetry measurements. The results obtained from the cyclic voltammetry measurements are consistent with that from the time-resolved fluorescence measurements. The possibility of the selected xanthene dye as an acceptor for the hole of the photoexcited C_3N_4 was also discussed.

EXPERIMENTAL SECTION

Chemicals and Sample Preparation. Fluorescein, dibromofluorescein, and eosin Y were purchased from Sigma-Aldrich Co. LLC and used as received. Erythrosine B was purchased from Tokyo Chemical Industry Co. Ltd. and used as received. The sample C_3N_4 synthesized at 600 °C from dicyandiamide was a generous gift from Prof. Xinchen Wang at Fuzhou University, China. The xanthene dye-sensitized-C_3N_4 composite was synthesized through putting a given amount of C_3N_4 in a certain concentration of a selected xanthene dye aqueous solution. After the suspension was stirred for 24 h in a black closet, the solid sample was harvest by centrifugation and dried in a vacuum oven at room temperature.

Experimental Methods. The UV−vis diffuse reflectance spectra were recorded on a Shimadzu UV-3600 spectrophotometer equipped with a diffuse reflectance accessory, where their absorption spectra were referenced to $BaSO_4$. The X-ray diffraction patterns were recorded on a Shimadzu XRD-7000 diffractometer using Cu Kα as the X-ray radiation (λ = 1.54056 Å) under 40 kV and 30 mA. The cyclic voltammograms were recorded on a BAS ECepsilon electrochemistry workstation. In the cyclic voltammetry measurement, a three-electrode system was used, which includes a bare glassy carbon electrodes (diameter = 3.0 mm) as a working electrode, an Ag/AgCl electrode as a reference electrode, and a platinum wire as a counter electrode. The fluorescence decays were measured using a homemade time correlated single photon counting apparatus. Briefly, the second harmonic (395 nm) of the output of a Spectra Physics 1 kHz amplified Ti:sapphire laser or the output (460−560 nm) of an OPA pumped by a Spectra Physics 1 kHz amplified Ti:sapphire laser was used as the excitation source. The emission was collected and sent into a Princeton Instruments SP2358 monochromator and detected with a Hamamatsu R3809U-50 MCP-PMT. Next the signal from the R3809U-50 MCP-PMT was amplified by a Becher & Hickl GmbH HFAC-26 preamplifier. Then the output of the HFAC-26 preamplifier and the output of a fast PicoQuant TDA 200 photodiode were, respectively, connected to a Becher & Hickl GmbH SPC-130 module as the start and stop pulses. The instrumental response function (IRF) of this setup was about 70 ps.

RESULTS AND DISCUSSION

Figure 1 shows the UV−vis diffuse reflectance spectra and X-ray diffraction patterns of fluorescein-C_3N_4, dibromofluorescein-C_3N_4, eosin Y-C_3N_4, and erythrosine B-C_3N_4 composites. The UV−vis diffuse reflectance spectrum and X-ray diffraction pattern of C_3N_4 alone were also shown in Figure 1 as references. From Figure 1A, it is found that all selected xanthene dyes can extend the visible light response range of C_3N_4. The C_3N_4 sensitized with erythrosine B has the strongest absorption in the visible wavelength region, while the C_3N_4 sensitized with fluorescein has the weakest absorption in the visible wavelength region.

To understand the interaction between each selected xanthene dye and C_3N_4 in their corresponding dye-sensitized-C_3N_4 composites, we determined the maximal adsorption amount of each selected xanthene dye by C_3N_4 through measuring the absorbance change of each selected dye solution induced by adding a given amount of C_3N_4. It is derived that

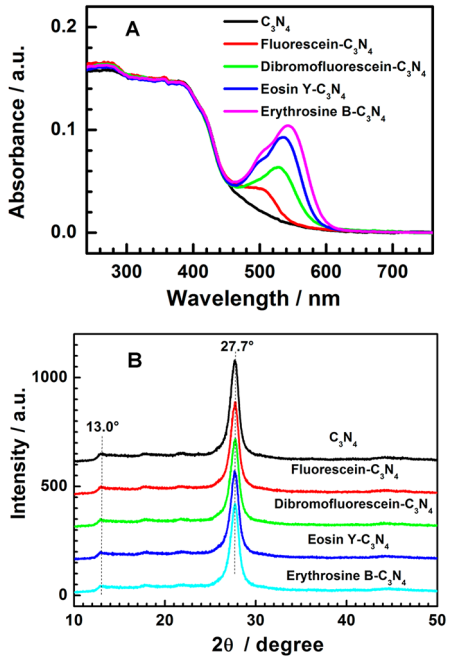

Figure 1. UV−vis diffuse reflectance spectra (A) and X-ray diffraction patterns (B) of C_3N_4 alone, fluorescein-C_3N_4, dibromofluorescein-C_3N_4, eosin Y-C_3N_4, and erythrosine B-C_3N_4 composites.

the maximal adsorption amount of fluorescein, dibromofluorescein, eosin Y, and erythrosine B by C_3N_4 is 4.4, 3.2, 7.3, and 8.6 μmol g^{-1}, respectively. The obtained 7.3 μmol g^{-1} for eosin Y adsorbed by C_3N_4 agrees well with the reported value of 7.66 μmol g^{-1} by Xu et al.[24] The small values of the obtained adsorption amount for each selected xanthene dye by C_3N_4 agree with the X-ray diffraction measurements of fluorescein-C_3N_4, dibromofluorescein-C_3N_4, eosin Y-C_3N_4, and erythrosine B-C_3N_4 composites (Figure 1B), where each selected xanthene dye-sensitized-C_3N_4 composite has an almost identical X-ray diffraction pattern to that of C_3N_4 alone. The strong peak located at around 27.7° 2θ is generally assigned to the (002) stacking of polymeric or graphitic sheets,[25] which corresponds to about a 0.322 nm repeat distance. The weak peak located at around 13.0° 2θ is related to an in-plane structural packing motif,[26] which corresponds to about a 0.680 nm repeat distance.

To find out whether the electron on the LUMO of each selected photoexcited xanthene dye can be transferred to the conduction band of C_3N_4 or not, we systematically recorded the fluorescence decays of fluorescein, dibromofluorescein, eosin Y, and erythrosine B in their corresponding saturated dye aqueous solutions (Figure 2A) and in their corresponding dye-sensitized-C_3N_4 composites (Figure 2B) with picosecond time-resolved fluorescence measurements. The excitation wavelength was chosen at 515 nm for fluorescein-C_3N_4, 530 nm for dibromofluorescein-C_3N_4, 535 nm for eosin Y-C_3N_4, and 545 nm for erythrosine B-C_3N_4, respectively. The fluorescence decays of fluorescein, dibromofluorescein, eosin Y, and erythrosine B in their saturated dye aqueous solutions (Figure 2A) can be fitted with a single exponential decay function, while the fluorescence decays of fluorescein, dibromofluorescein, eosin Y, and erythrosine B in their dye-sensitized-C_3N_4 composites (Figure 2B) need a summation of two exponential decay functions to be fitted. Table 1 summarized all fitting parameters for the fluorescence decays of fluorescein,

DOI: 10.1021/acsami.5b06309
ACS Appl. Mater. Interfaces 2015, 7, 21868−21874

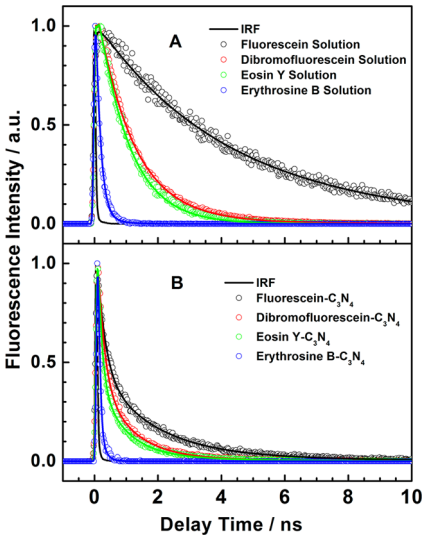

Figure 2. Fluorescence decays of fluorescein, dibromofluorescein, eosin Y, and erythrosine B in their corresponding saturated dye aqueous solutions (A) and in their corresponding dye-sensitized-C_3N_4 (fluorescein-C_3N_4, dibromofluorescein-C_3N_4, eosin Y-C_3N_4, and erythrosine B-C_3N_4) composites (B).

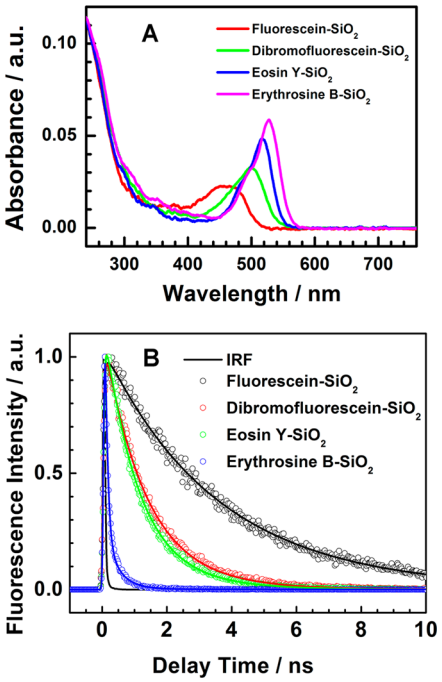

Figure 3. (A) UV−vis diffuse reflectance spectra of fluorescein-SiO_2, dibromofluorescein-SiO_2, eosin Y-SiO_2, and erythrosine B-SiO_2 composites. (B) Fluorescence decays of fluorescein, dibromofluorescein, eosin Y, and erythrosine B in their corresponding dye-SiO_2 (fluorescein-SiO_2, dibromofluorescein-SiO_2, eosin Y-SiO_2, and erythrosine B-SiO_2) composites.

dibromofluorescein, eosin Y, and erythrosine B in their saturated dye aqueous solutions and in their dye-sensitized-C_3N_4 composites.

It is clear that the averaged fluorescence lifetime ($\langle\tau\rangle$) of each selected xanthene dye in their corresponding dye-sensitized-C_3N_4 composite is obviously shorter than that in their corresponding saturated dye aqueous solution. Two reasons could shorten the fluorescence lifetime of each selected xanthene dye in its corresponding dye-sensitized-C_3N_4 composite, one is the dye aggregation on the surface of C_3N_4 and the other is the electron transfer from the LUMO of the photoexcited xanthene dye to the conduction band of C_3N_4. To get rid of the effect of the dye aggregation on the fluorescence lifetime shortening of each selected xanthene dye in their corresponding dye-sensitized-C_3N_4 composites, we further prepared their corresponding dye-SiO_2 composite (no electron transfer occurs) as reference and measured the fluorescence decays of each selected xanthene dye in their corresponding dye-SiO_2 composites. Figure 3A shows the UV−vis diffuse reflectance spectra of fluorescein-SiO_2, dibromofluorescein-SiO_2, eosin Y-SiO_2, and erythrosine B-SiO_2 composites, and Figure 3B displays the fluorescence decays of fluorescein, dibromofluorescein, eosin Y, and erythrosine B in fluorescein-SiO_2, dibromofluorescein-SiO_2, eosin Y-SiO_2, and erythrosine B-SiO_2 composites. From Figure 3A, it can be found that the maximal adsorption amount of fluorescein, dibromofluorescein, eosin Y, and erythrosine B by SiO_2 is quite similar to that by C_3N_4. Besides, we determined the Brunauer−Emmett−Teller (BET) surface areas of C_3N_4 and SiO_2 through measuring their nitrogen adsorption−desorption isotherms at 77 K using a Micromeritics Tristar II 3020 equipment and found that the BET surface areas of C_3N_4 and SiO_2 are not much different (~25 m^2/g for C_3N_4 and ~60 m^2/g for SiO_2). This indicates that the aggregation behavior of each selected xanthene dye on the surface of C_3N_4 is not much different with that on the surface of SiO_2. However, from the data shown in Figure 2B and Figure 3B, it is found that the fluorescence decays of fluorescein, dibromofluorescein, eosin Y, and erythrosine B in their corresponding dye-SiO_2 composites are obviously slower than the fluorescence decays of fluorescein, dibromofluorescein, eosin Y, and erythrosine B in their corresponding dye-sensitized-C_3N_4 composites. Meanwhile from the data shown in Figure 2A and Figure 3B, it is also found the fluorescence decays of fluorescein, dibromofluorescein, eosin Y, and erythrosine B in their corresponding dye-SiO_2 composites are

Table 1. Fitting Parameters for the Fluorescence Decay of Fluorescein, Dibromofluorescein, Eosin Y, and Erythrosine B in Their Saturated Dye Solutions, Dye-Sensitized-C_3N_4 Composites, and Dye-SiO_2 Composites

	fluorescein			dibromofluorescein			eosin Y			erythrosine B		
items	soln	C_3N_4	SiO_2	soln	C_3N_4	SiO_2	soln	C_3N_4	SiO_2	soln	C_3N_4	SiO_2
a_1[a]	1.00	0.39	1.00	1.00	0.29	1.00	1.00	0.24	1.00	1.00	0.05	1.0
τ_1[a]/ns	4.20	2.10	3.75	1.25	1.23	1.30	1.10	1.15	1.10	0.16	0.16	0.14
a_2[a]		0.61			0.71			0.76			0.95	
τ_2[a]/ns		0.32			0.25			0.20			0.11	
$\langle\tau\rangle$[b]/ns	4.20	1.04	3.75	1.25	0.54	1.30	1.10	0.43	1.10	0.16	0.11	0.14

[a]The errors for both the amplitudes and time constants are less than 5%. [b]$\langle\tau\rangle = \Sigma_i a_i\tau_i/\Sigma_i a_i$.

DOI: 10.1021/acsami.5b06309
ACS Appl. Mater. Interfaces 2015, 7, 21868−21874

almost identical to the fluorescence decays of fluorescein, dibromofluorescein, eosin Y, and erythrosine B in their saturated dye aqueous solutions. These experimental observations indicate that the shortening of the fluorescence time of fluorescein, dibromofluorescein, eosin Y, and erythrosine B in their respective dye-sensitized-C_3N_4 composites are not due to the aggregation of the xanthene dye on the surface of C_3N_4. Thus, the electron transfer from the LUMO of the photoexcited xanthene dye to the conduction band of C_3N_4 should be attributed to the shorter fluorescence time of fluorescein, dibromofluorescein, eosin Y, and erythrosine B in their corresponding dye-sensitized-C_3N_4 composites.

The fluorescence decays of fluorescein, dibromofluorescein, eosin Y, and erythrosine B in their corresponding dye-SiO_2 composites can also be fitted with a single exponential decay and their fitting parameters are also summarized in Table 1. With the data listed in Table 1, we derived that the electron transfer rates (k_{ET}, $k_{ET} = 1/\tau_{dye\text{-}C_3N_4} - 1/\tau_{dye\text{-}SiO_2}$) from the LUMO of the photoexcited fluorescein, dibromofluorescein, eosin Y, and erythrosine B to the conduction band of C_3N_4 are 0.7×10^9, 1.1×10^9, 1.4×10^9, and 1.9×10^9 s^{-1}, respectively. To our knowledge, this is the first time-resolved study on a dye-sensitized-C_3N_4 system to catch the electron transfer process from the LUMO of a photoexcited dye to the conduction band of C_3N_4. It is clear that the determined electron transfer rate from the LUMO of each photoexcited xanthene dye to the conduction band of C_3N_4 is much slower than the electron transfer rate from the LUMO of a photoexcited xanthene dye to the conduction band of TiO_2.[27,28] Three reasons could lead to this phenomenon: the first is that the interaction coupling between the xanthene dye and C_3N_4 is weaker than that between the xanthene dye and TiO_2, the second is that the driving force (ΔG) for the electron transfer reaction between the xanthene dye and C_3N_4 is smaller than that between the xanthene dye and TiO_2, and the third is that the time-resolution of our experimental apparatus (70 ps) is low so as to we may not catch all ultrafast electron transfer processes. To fully understand the electron transfer process from the LUMO of a photoexcited xanthene dye to the conduction band of C_3N_4, it requires a femtosecond time-resolved study on the xanthene dye-sensitized-C_3N_4 systems. Unfortunately, we can not perform such measurement (either a femtosecond transient absorption or a femtosecond transient fluorescence) at the current due to the difficulty to produce a C_3N_4 sample having near-optical quality.[29−31] Thus, the determined electron transfer rate with the current 70 ps time-resolved fluorescence measurement should be the slowest electron transfer rate (lower limit) from the LUMO of photoexcited xanthene dye to the conduction band of C_3N_4. The study presented here suggests that the electron on the LUMO of each selected photoexcited xanthene dye can be transferred to the conduction band of C_3N_4 and that the selected xanthene dye can be used as a sensitizer for C_3N_4 in their corresponding dye-sensitized-C_3N_4 composites. The xanthene dye as a sensitizer of C_3N_4 can extend the visible light absorption of C_3N_4 and increase its photocatalytic hydrogen evolution efficiency under visible light irradiation.

To give other evidence that the electron on the LUMO of the photoexcited xanthene dye can be transferred to the conduction band of C_3N_4 in its dye-sensitized-C_3N_4 composite, we further obtained the reduction potentials of each selected xanthene dye and C_3N_4 with cyclic voltammetry measurements. Figure 4 shows the cyclic voltammograms of fluorescein, dibromofluorescein, eosin Y, erythrosine B, and C_3N_4 in

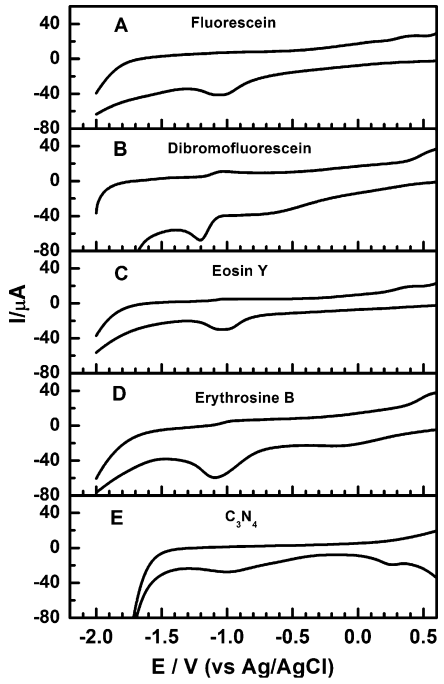

Figure 4. Cyclic voltammograms of fluorescein (A), dibromofluorescein (B), eosin Y (C), erythrosine B (D), and C_3N_4 (E) in aqueous solution.

aqueous solution. Clearly, fluorescein, dibromofluorescein, eosin Y, and erythrosine B displayed the reduction potential of −1.04, −1.20, −1.03, and −1.09 V vs Ag/AgCl, respectively, which corresponds to a LUMO energy of −3.66, −3.50, −3.67, and −3.61 eV (vs vacuum), respectively. The obtained reduction potentials for fluorescien, eosin Y, and erythrosine B all are consistent with the literature reports.[22,32,33] The C_3N_4 showed the reduction potential of −0.98 V vs Ag/AgCl, corresponding to a conduction band energy of −3.72 eV (vs vacuum), which is also consistent with the literature's report.[22] The level of the LUMO energy of all selected xanthene dyes are higher than that of the C_3N_4 conduction band energy, suggesting that the electron can be transferred from the LUMO of each selected photoexcited xanthene dye to the conduction band of C_3N_4 in their respective dye-sensitized-C_3N_4 composites. The cyclic voltammetry measurements gave a consistent result as the time-resolved fluorescence measurements.

With the obtained LUMO energy of each selected xanthene dye and the obtained conduction band energy of C_3N_4, we derived the driving force (ΔG) for the electron transfer process from the LUMO of the photoexcited fluorescein, dibromofluorescein, eosin Y, and erythrosine B to the conduction band of C_3N_4 is −0.06, −0.22, −0.05, and −0.11 eV, respectively. We also determined that the electron transfer rates from the LUMO of the photoexcited fluorescein, dibromofluorescein, eosin Y, and erythrosine B to the conduction band of C_3N_4 are 0.7×10^9, 1.1×10^9, 1.4×10^9, and 1.9×10^9 s^{-1}, respectively. It is clear that the increase of the electron transfer rate is not very well correlated with the driving force for the electron transfer from the LUMO of the photoexcited xanthene dye to the conduction band of C_3N_4 under Marcus electron transfer

DOI: 10.1021/acsami.5b06309
ACS Appl. Mater. Interfaces 2015, 7, 21868−21874

theory, indicating that either the interaction coupling between each selected xanthene dye and C_3N_4 are different or the electron transfer process from the LUMO of the photoexcited xanthene dye to the conduction band of C_3N_4 is faster than the time-resolution of our experimental apparatus. Since the obtained electron transfer rate is based on a low time-resolution (70 ps) fluorescence measurement, herein, we do not intend to provide a quantitative analysis of the relationship between electron transfer rate and energy difference in the context of Marcus electron transfer theory. Once we perform a femtosecond time-resolved study (either femtosecond transient absorption or femtosecond transient fluorescence) on these systems, we will provide a deep understanding of the electron transfer process from the LUMO of the photoexcited xanthene dye to the conduction band of C_3N_4. However, this is a big challenge for us currently due to the difficulty to produce a dye-sensitized-C_3N_4 sample having near-optical quality. Without a femtosecond time-resolved study, the results presented here still provide valuable information on the fundamental aspects of xanthene dye-sensitized-C_3N_4 photocatalytic systems.

In addition, with the obtained LUMO energy of fluorescein, dibromofluorescein, eosin Y, and erythrosine B and the obtained zero−zero transition energy of fluorescein, dibromofluorescein, eosin Y, and erythrosine B (Table S1 in the Supporting Information), we derived the energy of the HOMO of fluorescein, dibromofluorescein, eosin Y, and erythrosine B is −6.12, −5.91, −6.01, and −5.91 eV (vs vacuum), respectively. Similarly, with the obtained −3.72 eV (vs vacuum) conduction band energy and the reported 2.7 eV band gap of C_3N_4,[22,34] we derived the energy of the valence band of C_3N_4 is −6.42 eV (vs vacuum). The energy levels of the HOMO of all selected xanthene dyes are higher than the energy level of the valence band of C_3N_4, indicating that the electron on the HOMO of each selected xanthene dye can also be transferred to the valence band of the photoexcited C_3N_4. This means that the selected xanthene dye can also be used as an acceptor for the hole of the photoexcited C_3N_4 to increase the photocatalytic activity of C_3N_4. The role of a dye as an acceptor for the hole of a photoexcited quantum dot has been addressed in dye-sensitized quantum dot solar cell systems.[35−37] However, the role of a dye as an acceptor for the hole of the photoexcited C_3N_4 in a dye-sensitized-C_3N_4 system has not been reported in the literature. To confirm that the selected xanthene dye can be used as an acceptor for the hole of the photoexcited C_3N_4 in their corresponding dye-sensitized-C_3N_4 composite, we further recorded the fluorescence decays of C_3N_4 in fluorescein-C_3N_4, dibromofluorescein-C_3N_4, eosin Y-C_3N_4, and erythrosine B-C_3N_4 composites with 395 nm light excitation, as shown in Figure 5. The fluorescence decay of C_3N_4 alone was also shown in Figure 5 as a reference. The 395 nm light only excites C_3N_4.

The C_3N_4 in each selected xanthene dye-sensitized-C_3N_4 composite has a similar lifetime as the C_3N_4 alone does (Figure 5 and Table 2). None of the selected xanthene dye can shorten the fluorescence lifetime of C_3N_4 in fluorescein-C_3N_4, dibromofluorescein-C_3N_4, eosin Y-C_3N_4, and erythrosine B-C_3N_4 composite. This observation seems to disagree with the prediction from the energy level difference between the HOMO of each selected xanthene dye and the valence band of C_3N_4. However, it could be understandable why the C_3N_4 in its respective xanthene dye-sensitized-C_3N_4 composite has a similar fluorescence decay as the C_3N_4 alone does when one analyzes the weight percentage of each selected xanthene dye to C_3N_4 in their respective dye-sensitized-C_3N_4 composite. It is found that the maximal adsorption amounts of all selected xanthene dyes on the surface of C_3N_4 are less than 10 μmol g^{-1}. The 10 μmol g^{-1} adsorption amount of xanthene dye by C_3N_4 corresponds to introducing a less than 1% w/w impurity for the C_3N_4 sample. A less than 1% w/w impurity adding to the C_3N_4 sample can not provide an observable change on the fluorescence lifetime of C_3N_4 in its corresponding dye-sensitized-C_3N_4 composite. Although we did not observe the fluorescence lifetime change of C_3N_4 in its corresponding dye-sensitized-C_3N_4 composite (Figure 5), we still suggest that the electron on the HOMO of each selected xanthene dye can transfer to the photoexcited C_3N_4 valence band on the basis of the prediction from their energy level location. The electron transfer from the HOMO of the selected xanthene dye to the photoexcited C_3N_4 valence band would also retard the lifetime of the electron on the conduction band of the photoexcited C_3N_4, which would benefit to increasing the photocatalytic hydrogen evolution efficiency of C_3N_4 under a certain wavelength range of light irradiation.

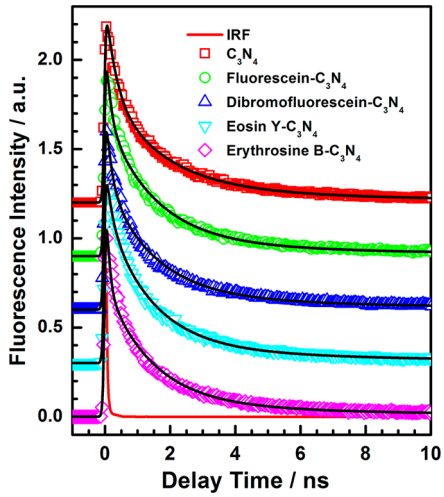

Figure 5. Fluorescence decays of C_3N_4 in C_3N_4 alone, fluorescein-C_3N_4, dibromofluorescein-C_3N_4, eosin Y-C_3N_4, and erythrosine B-C_3N_4 composites. Excitation wavelength, 395 nm; detection wavelength, 470 nm.

CONCLUSIONS

In summary, we have carried a systematic study on the interaction dynamics between C_3N_4 and several selected xanthene dyes such as fluorescein, dibromofluorescein, eosin Y, and erythrosine B in their respective dye-sensitized-C_3N_4 composite using both time-resolved fluorescence spectroscopy and cyclic voltammetry experiments. Both the time-resolved fluorescence and the cyclic voltammetry measurements suggest that the electron on the LUMO of each selected photoexcited xanthene dye can be transferred to the conduction band of C_3N_4 in their corresponding dye-sensitized-C_3N_4 composites. With a 70 ps time-resolved fluorescence apparatus, we determined the slowest electron transfer rates from the LUMO of the photoexcited fluorescein, dibromofluorescein, eosin Y, and erythrosine B to the conduction band of C_3N_4 are 0.7×10^9, 1.1×10^9, 1.4×10^9, and 1.9×10^9 s^{-1}, respectively, in their corresponding dye-sensitized-C_3N_4 composites. The current study is significant for the researcher understanding of the fundamental aspects in the xanthene dye-sensitized-C_3N_4 photocatalytic systems.

DOI: 10.1021/acsami.5b06309
ACS Appl. Mater. Interfaces 2015, 7, 21868−21874

Table 2. Fitting Parameters for the Fluorescence Decay of C_3N_4 in C_3N_4 Alone, Fluorescein-C_3N_4, Dibromofluorescein-C_3N_4, Eosin Y-C_3N_4, and Erythrosine B-C_3N_4 Composites[a]

sample	a_1[b]	τ_1[c]/ns	a_2[b]	τ_2[c]/ns	a_3[b]	τ_3[c]/ns	$\langle\tau\rangle$[d]/ns
C_3N_4	0.09	0.20	0.56	1.66	0.35	8.25	3.84
fluorescein-C_3N_4	0.05	0.13	0.60	1.50	0.34	8.62	3.84
dibromofluorescein-C_3N_4	0.06	0.16	0.58	1.47	0.36	8.29	3.85
eosin Y-C_3N_4	0.04	0.17	0.59	1.39	0.37	8.06	3.81
erythrosine B-C_3N_4	0.06	0.12	0.59	1.42	0.35	8.28	3.74

[a]Excitation wavelength: 395 nm. Detection wavelength: 470 nm. [b]The errors for the amplitudes are less than 10%. [c]The errors for the time constants are less than 5%. [d]$\langle\tau\rangle = \Sigma_i a_i\tau_i/\Sigma_i a_i$.

■ ASSOCIATED CONTENT

Supporting Information

The Supporting Information is available free of charge on the ACS Publications website at DOI: 10.1021/acsami.5b06309.

Additional spectra and spectroscopic data (PDF)

■ AUTHOR INFORMATION

Corresponding Author

*Phone: +86-10-6251-4601. Fax: +86-10-6251-6444. E-mail: a.yu@chem.ruc.edu.cn.

Notes

The authors declare no competing financial interest.

■ ACKNOWLEDGMENTS

This work was supported by the National Natural Science Foundation of China (Grant 21373269).

■ REFERENCES

(1) Ge, L.; Han, C. C.; Liu, J.; Li, Y. F. Enhanced Visible Light Photocatalytic Activity of Novel Polymeric g-C3N4 Loaded with Ag Nanoparticles. *Appl. Catal., A* **2011**, *409−410*, 215−222.

(2) Maeda, K.; Domen, K. New Non-Oxide Photocatalysts Designed for Overall Water Splitting under Visible Light. *J. Phys. Chem. C* **2007**, *111*, 7851−7861.

(3) Zhang, J. H.; Zhang, G. G.; Chen, X. F.; Lin, S.; Möhlmann, L.; Dołęga, G.; Lipner, G.; Antonietti, M.; Blechert, S.; Wang, X. C. Co-Monomer Control of Carbon Nitride Semiconductors to Optimize Hydrogen Evolution with Visible Light. *Angew. Chem.* **2012**, *124*, 3237−3241.

(4) Zhang, J. S.; Sun, J. H.; Maeda, K.; Domen, K.; Liu, P.; Antonietti, M.; Fu, X. Z.; Wang, X. C. Sulfur-Mediated Synthesis of Carbon Nitride: Band-Gap Engineering and Improved Functions for Photocatalysis. *Energy Environ. Sci.* **2011**, *4*, 675−678.

(5) Wang, X. C.; Maeda, K.; Thomas, A.; Takanabe, K.; Xin, G.; Carlsson, J. M.; Domen, K.; Antonietti, M. A Metal-Free Polymeric Photocatalyst for Hydrogen Production From Water under Visible Light. *Nat. Mater.* **2009**, *8*, 76−80.

(6) Wang, X. C.; Maeda, K.; Chen, X. F.; Takanabe, K.; Domen, K.; Hou, Y. D.; Fu, X. Z.; Antonietti, M. Polymer Semiconductors for Artificial Photosynthesis: Hydrogen Evolution by Mesoporous Graphitic Carbon Nitride with Visible Light. *J. Am. Chem. Soc.* **2009**, *131*, 1680−1681.

(7) Cao, S. W.; Yu, J. G. g-C3N4-Based Photocatalysts for Hydrogen Generation. *J. Phys. Chem. Lett.* **2014**, *5*, 2101−2107.

(8) Martin, D. J.; Reardon, P. J. T.; Moniz, S. J. A.; Tang, J. W. Visible Light-Driven Pure Water Splitting by a Nature-Inspired Organic Semiconductor-Based System. *J. Am. Chem. Soc.* **2014**, *136*, 12568−12571.

(9) Sui, Y.; Liu, J. H.; Zhang, Y. W.; Tian, X. K.; Chen, W. Dispersed Conductive Polymer Nanoparticles on Graphitic Carbon Nitride for Enhanced Solar-Driven Hydrogen Evolution from Pure Water. *Nanoscale* **2013**, *5*, 9150−9155.

(10) Wang, Y.; Di, Y.; Antonietti, M.; Li, H. R.; Chen, X. F.; Wang, X. C. Excellent Visible-Light Photocatalysis of Fluorinated Polymeric Carbon Nitride Solids. *Chem. Mater.* **2010**, *22*, 5119−5121.

(11) Yan, S. C.; Li, Z. S.; Zou, Z. G. Photodegradation Performance of g-C3N4 Fabricated by Directly Heating Melamine. *Langmuir* **2009**, *25*, 10397−10401.

(12) Wang, X. C.; Chen, X. F.; Thomas, A.; Fu, X. Z.; Antonietti, M. Metal-Containing Carbon Nitride Compounds: A New Functional Organic−Metal Hybrid Material. *Adv. Mater.* **2009**, *21*, 1609−1612.

(13) Yu, J. G.; Wang, S. H.; Cheng, B.; Lin, Z.; Huang, F. Noble Metal-Free Ni(OH)2-g-C3N4 Composite Photocatalyst with Enhanced Visible-Light Photocatalytic H2-Production Activity. *Catal. Sci. Technol.* **2013**, *3*, 1782−1789.

(14) Chen, X. F.; Jun, Y.-S.; Takanabe, K.; Maeda, K.; Domen, K.; Fu, X. Z.; Antonietti, M.; Wang, X. C. Ordered Mesoporous SBA-15 Type Graphitic Carbon Nitride: A Semiconductor Host Structure for Photocatalytic Hydrogen Evolution with Visible Light. *Chem. Mater.* **2009**, *21*, 4093−4095.

(15) Zhang, H. Y.; Yu, A. C. Photophysics and Photocatalysis of Carbon Nitride Synthesized at Different Temperatures. *J. Phys. Chem. C* **2014**, *118*, 11628−11635.

(16) Takanabe, K.; Kamata, K.; Wang, X. C.; Antonietti, M.; Kubota, J.; Domen, K. Photocatalytic Hydrogen Evolution on Dye-Sensitized Mesoporous Carbon Nitride Photocatalyst with Magnesium Phthalocyanine. *Phys. Chem. Chem. Phys.* **2010**, *12*, 13020−13025.

(17) Zhang, X. H.; Yu, L. J.; Zhuang, C. S.; Peng, T. Y.; Li, R. J.; Li, X. G. Highly Asymmetric Phthalocyanine as a Sensitizer of Graphitic Carbon Nitride for Extremely Efficient Photocatalytic H2 Production under Near-Infrared Light. *ACS Catal.* **2014**, *4*, 162−170.

(18) Zhang, X. H.; Yu, L. J.; Li, R. J.; Peng, T. Y.; Li, X. G. Asymmetry and Electronic Directionality: A Means of Improving the Red/Near-IR-Light-Responsive Photoactivity of Phthalocyanine-Sensitized Carbon Nitride. *Catal. Sci. Technol.* **2014**, *4*, 3251−3260.

(19) Yu, L. J.; Zhang, X. H.; Zhuang, C. S.; Lin, L.; Li, R. J.; Peng, T. Y. Syntheses of Asymmetric Zinc Phthalocyanines as Sensitizer of Pt-loaded Graphitic Carbon Nitride for Efficient Visible/Near-IR-Light-Driven H2 Production. *Phys. Chem. Chem. Phys.* **2014**, *16*, 4106−4114.

(20) Zhang, X. H.; Peng, T. Y.; Yu, L. J.; Li, R. J.; Li, Q. Q.; Li, Z. Visible/Near-Infrared-Light-Induced H-2 Production over g-C3N4 Co-sensitized by Organic Dye and Zinc Phthalocyanine Derivative. *ACS Catal.* **2015**, *5*, 504−510.

(21) Min, S. X.; Lu, G. X. Enhanced Electron Transfer from the Excited Eosin Y to mpg-C3N4 for Highly Efficient Hydrogen Evolution under 550 nm Irradiation. *J. Phys. Chem. C* **2012**, *116*, 19644−19652.

(22) Wang, Y. B.; Hong, J. D.; Zhang, W.; Xu, R. Carbon Nitride Nanosheets for Photocatalytic Hydrogen Evolution: Remarkably Enhanced Activity by Dye Sensitization. *Catal. Sci. Technol.* **2013**, *3*, 1703−1711.

(23) Li, Q. Y.; Yue, B.; Iwai, H.; Kako, T.; Ye, J. H. Carbon Nitride Polymers Sensitized with N-Doped Tantalic Acid for Visible Light-Induced Photocatalytic Hydrogen Evolution. *J. Phys. Chem. C* **2010**, *114*, 4100−4105.

(24) Xu, J. J.; Li, Y. X.; Peng, S. Q.; Lu, G. X.; Li, S. B. Eosin Y-Sensitized Graphitic Carbon Nitride Fabricated by Heating Urea for Visible Light Photocatalytic Hydrogen Evolution: The Effect of the

DOI: 10.1021/acsami.5b06309
ACS Appl. Mater. Interfaces 2015, 7, 21868−21874

Pyrolysis Temperature of Urea. *Phys. Chem. Chem. Phys.* **2013**, *15*, 7657−7665.
(25) Jorge, A. B.; Martin, D. J.; Dhanoa, M. T. S.; Rahman, A. S.; Makwana, N.; Tang, J.; Sella, A.; Cora, F.; Firth, S.; Darr, J. A.; McMillan, P. F. H-2 and O-2 Evolution from Water Half-Splitting Reactions by Graphitic Carbon Nitride Materials. *J. Phys. Chem. C* **2013**, *117*, 7178−7185.
(26) Thomas, A.; Fischer, A.; Goettmann, F.; Antonietti, M.; Muller, J.-O.; Schlogl, R.; Carlsson, J. M. Graphitic Carbon Nitride Materials: Variation of Structure and Morphology and Their Use as Metal-Free Catalysts. *J. Mater. Chem.* **2008**, *18*, 4893−4908.
(27) Benko, G.; Hilgendorff, M.; Yartsev, A. P.; Sundstrom, V. Electron Injection and Recombination in Fluorescein 27-Sensitized TiO2 Thin Films. *J. Phys. Chem. B* **2001**, *105*, 967−974.
(28) Ramakrishna, G.; Ghosh, H. N. Emission From the Charge Transfer State of Xanthene Dye-Sensitized TiO2 Nanoparticles: A New Approach to Determining Back Electron Transfer Rate and Verifying the Marcus Inverted Regime. *J. Phys. Chem. B* **2001**, *105*, 7000−7008.
(29) Gillan, E. G. Synthesis of Nitrogen-Rich Carbon Nitride Networks from an Energetic Molecular Azide Precursor. *Chem. Mater.* **2000**, *12*, 3906−3912.
(30) Shi, Y. Q.; Jiang, S. H.; Zhou, K. Q.; Bao, C. L.; Yu, B.; Qian, X. D.; Wang, B. B.; Hong, N. N.; Wen, P. Y.; Gui, Z.; Hu, Y.; Yuen, R. K. K. Influence of g-C3N4 Nanosheets on Thermal Stability and Mechanical Properties of Biopolymer Electrolyte Nanocomposite Films: A Novel Investigation. *ACS Appl. Mater. Interfaces* **2014**, *6*, 429−437.
(31) Zhang, Y. J.; Thomas, A.; Antonietti, M.; Wang, X. C. Activation of Carbon Nitride Solids by Protonation: Morphology Changes, Enhanced Ionic Conductivity, and Photoconduction Experiments. *J. Am. Chem. Soc.* **2009**, *131*, 50−51.
(32) Urano, Y.; Kamiya, M.; Kanda, K.; Ueno, T.; Hirose, K.; Nagano, T. Evolution of Fluorescein as a Platform for Finely Tunable Fluorescence Probes. *J. Am. Chem. Soc.* **2005**, *127*, 4888−4894.
(33) Zhang, J.; Sun, L.; Yoshida, T. Spectroelectrochemical Studies on Redox Reactions of Eosin Y and Its Polymerization with Zn2+ Ions. *J. Electroanal. Chem.* **2011**, *662*, 384−395.
(34) Wang, Y.; Wang, X. C.; Antonietti, M. Polymeric Graphitic Carbon Nitride as a Heterogeneous Organocatalyst: From Photochemistry to Multipurpose Catalysis to Sustainable Chemistry. *Angew. Chem., Int. Ed.* **2012**, *51*, 68−89.
(35) Choi, H.; Kamat, P. V. CdS Nanowire Solar Cells: Dual Role of Squaraine Dye as a Sensitizer and a Hole Transporter. *J. Phys. Chem. Lett.* **2013**, *4*, 3983−3991.
(36) Maity, P.; Debnath, T.; Ghosh, H. N. Ultrafast Hole- and Electron-Transfer Dynamics in CdS-Dibromofluorescein (DBF) Supersensitized Quantum Dot Solar Cell Materials. *J. Phys. Chem. Lett.* **2013**, *4*, 4020−4025.
(37) Singhal, P.; Ghosh, H. N. Ultrafast Hole/Electron Transfer Dynamics in a CdSe Quantum Dot Sensitized by Pyrogallol Red: A Super-Sensitization System. *J. Phys. Chem. C* **2014**, *118*, 16358−16365.

DOI: 10.1021/acsami.5b06309
ACS Appl. Mater. Interfaces 2015, 7, 21868−21874